EARTH SURFACE PROCESSES AND LANDFORMS
Earth Surf. Process. Landforms **38**, 1725–1734 (2013)

Published online 10 July 2013 in Wiley Online Library
(wileyonlinelibrary.com) DOI: 10.1002/esp.3459

Effect of natural restoration time of abandoned farmland on soil detachment by overland flow in the Loess Plateau of China

Bing Wang,[1,2] Guang-hui Zhang,[1,2]* Yang-yang Shi,[1,3] X.C. Zhang,[4] Zong-ping Ren[2] and Liang-jun Zhu[2]
[1] State Key Laboratory of Soil Erosion and Dryland Farming on the Loess Plateau, Institute of Water and Soil Conservation, Chinese Academy of Sciences and Ministry of Water Resources, Yangling, Shaanxi, 712100, China
[2] School of Geography, Beijing Normal University, Beijing, 100875, China
[3] College of Forestry, Northwest A & F University, Yangling, Shaanxi, 712100, China
[4] USDA ARS, Grazinglands Res Lab, El Reno, OK, USA

Received 29 May 2012; Revised 6 June 2013; Accepted 10 June 2013

*Correspondence to: Guang-Hui Zhang, School of Geography, Beijing Normal University, Beijing, 100875, China. E-mail: ghzhang@bnu.edu.cn

ESPL
Earth Surface Processes and Landforms

ABSTRACT: Vegetation restoration has significant effects on soil properties and vegetation cover and thus affects soil detachment by overland flow. Few studies have been conducted to evaluate this effect in the Loess Plateau where a Great Green Project was implemented in the past decade. This study was carried out to quantify the effects of age of abandoned farmland under natural vegetation restoration on soil detachment by overland flow and soil resistance to erosion as reflected by soil erodibility and critical shear stress. The undisturbed soil samples were collected from five abandoned farmlands with natural restoration age varying from 3 to 37 years. The samples were subjected to flow scouring in a 4.0 m long by 0.35 m wide hydraulic flume under six different shear stresses ranging from 5.60 to 18.15 Pa. The results showed that the measured soil detachment capacities in currently cultivated farmland were 24.1 to 35.4 times greater than those of the abandoned farmlands. For the abandoned farmlands, soil detachment capacities fluctuated greatly due to the complex effects of root density and biological crust thickness, and could be simulated well by flow shear stress and biological crust thickness with a power function (NSE = 0.851). Soil erodibility of abandoned farmlands decreased gradually with restoration age and reached a steady stage when restoration age was greater than 28 years. The critical shear stress of the natural abandoned farmlands declined when restoration age was less than 18 years and then increased due to the episodic influences of vegetation recovery and biological crust development. More studies in the Loess Plateau are necessary to quantify the relationship between soil detachment capacity and biological crust thickness for better understanding the mechanism of soil detachment under natural vegetation restoration. Copyright © 2013 John Wiley & Sons, Ltd.

KEYWORDS: soil erosion; flow detachment; vegetation; restoration age; Loess Plateau

Introduction

The Loess Plateau is one of the mostly severely eroded regions in the world. Severe erosion by water is caused by frequent heavy storms, steep slopes, easily eroded silty loam soils, scarce vegetation, and intense human activities. The mean annual soil erosion rates ranged from 5000 to 10 000 tonnes km^{-2} yr^{-1} (Fu and Gulinck, 1994; Zhang and Liu, 2005; Zhang *et al.*, 2008b). Such serious soil erosion has slowed down socio-economic and environmental development by its direct and indirect influence in this region. The Chinese government realized the seriousness of this issue and began to implement a series of biological and engineering measures and conservation tillage practices in the Loess Plateau in order to achieve sustainable development of the socio-economic environment by controlling soil erosion and restoring the disturbed ecosystem (Li *et al.*, 2012; Zhang *et al.*, 2008b).

Govers *et al.* (1990) defined soil erosion by overland flow as the detachment and displacement of soil particles by overland flow. Describing soil detachment from land surface mathematically is an essential process of soil erosion modeling (Laflen *et al.*, 1991). Different relationships for soil detachment by overland flow are used in soil erosion models to estimate initiation and rates of erosion by scouring in rills. These models are usually quite sensitive to both rill erosion rates and rill flow hydraulics used to describe soil detachment in a rill (Govers *et al.*, 2007). Many experiments have been conducted in past decades to study the mechanism of soil detachment by overland flow. Results indicate that soil detachment is strongly influenced by hydraulic parameters of overland flow, such as flow regime, discharge, slope gradient, flow depth, velocity, friction, and sediment concentration (Govers *et al.*, 1990; Cochrane and Flanagan, 1997; Nearing *et al.*, 1999; Zhang *et al.*, 2002, 2003). In process-based erosion models, hydraulic parameters of shear stress (Nearing *et al.*, 1991), stream power (Hairsine and Rose, 1992a, 1992b; Zhang *et al.*, 2002, 2003), and unit stream power (Morgan *et al.*, 1998) are normally used to simulate soil detachment processes.

Soil properties have strong effects on soil detachment by overland flow. Recent studies showed that soil detachment was closely related to soil type, texture, bulk density, cohesion, clay content, organic matter content, soil moisture, and infiltration rate (Khanbilvardi and Rogowski, 1986; Nearing *et al*., 1988; Ghebreiyessus *et al*., 1994; Morgan *et al*., 1998; Zheng *et al*., 2000). Torri *et al*. (1998) found that soil detachment capacity increased as dry soil bulk density and aggregate median diameter increased, whereas it decreased as clay content and soil strength increased. Knapen *et al*. (2008) reported that soil detachment capacity decreased with increase in soil water content and organic matter. Any change in soil properties produced by farming activities, land use adjustment, soil consolidation, and vegetation growth certainly would result in changes in soil detachment by overland flow (Zhang *et al*., 2008a, 2009).

Vegetation root networks probably play a great role in protecting soil against water erosion and enhance its stability by binding soil particles and aggregates (De Baets *et al*., 2006), and thus reduce soil detachment. Root protection is even more important in semi-arid environments, where vegetation coverage is sparse and seasonal. De Baets *et al*. (2007) reported that the effect of roots on erosion reduction during an overland flow event was more profound than that indicated in previous studies (Wischmeier, 1975; Dissmeyer and Foster, 1980). Different root variables (e.g. mass density, length density, surface area density, dry weight, area ratio, and diameter) were used to predict the erosion-reducing effects of roots on soil detachment capacities by overland flow (Li *et al*., 1991; Mamo and Bubenzer, 2001a, 2001b; Zhou and Shang-Guan, 2005; De Baets *et al*., 2006, 2007). The influences of root system on soil detachment capacity were also related to root architectures. Some studies showed that tap roots, compared with fibrous roots, were less effective in reducing erosion rates (Wischmeier, 1975; Dissmeyer and Foster, 1980; De Baets *et al*., 2007).

Farmland is a principal sediment source in the Loess Plateau since it is the predominant eroded land use type in this region, and the average detachment capacity is 2.05 to 13.32 times greater than those of grassland, wasteland, shrub land, and woodland (Zhang *et al*., 2008a) caused by disturbance of farming activities (Zhang *et al*., 2003, 2009). Land use in the Loess Plateau has changed since several projects of ecological restoration were carried out in the 1970s to control soil erosion (Chen *et al*., 2007). Extensive tree planting on slope farmland (1970s) and integrated soil erosion control at watershed scales (1980s and 1990s) were carried out in the Loess Plateau. Between 1984 and 1996, slope farmland decreased by 43%, while forest land and grassland increased by 36% and 5%, respectively (Fu *et al*., 2000). However, soil erosion was still very severe on cultivated slope farmlands until the late 1990s when the project 'Grain for Green' was implemented. In this project, farmers were compensated with grain in exchange for taking their steep croplands ($> 25.9\%$) out of production and allowing natural vegetation recovery (passive restoration) (Fu *et al*., 2000).

Land use change in the Loess Plateau might have altered both soil properties and vegetation characteristics. Soil hydro-physical parameters such as infiltration, cohesion, water-holding capacity, soil porosity, bulk density, aggregate stability, and saturated hydraulic conductivity were closely related to land use conditions (Li *et al*., 1995; Liu *et al*., 2003; Li and Shao, 2006; Xu *et al*., 2006; Hu *et al*., 2008). Vegetation characteristics (e.g. coverage, community structure, and species composition and diversity) were also greatly affected by land use conversion (Jiang *et al*., 2003). Both changes in vegetation and soil property characteristics caused by land use adjustments are probably related to the chronosequence of natural vegetation restoration, and the particular mechanisms need to be investigated. With progression in natural restoration chronosequence, hydraulics characteristics, physical and chemical properties of soils, and vegetation characteristics changed greatly (Jiao *et al*., 2007; Zhu *et al*., 2009; Wang *et al*., 2011), certainly resulting in changes in soil detachment processes. However, the quantitative relationships between soil detachment capacity and plant restoration age are not known in the Loess plateau. The aims of this study were to quantify the effects of the age of natural restoration on soil detachment by overland flow following abandonment of steep farmland and to investigate the changes in soil resistance to erosion with restoration age as reflected by soil erodibility (K_r) and critical shear stress (τ_c) in the Loess Plateau of China.

Materials and Methods

Study area

The study was performed in the Zhifanggou small watershed (longitude 109°19′23″E, latitude 36°51′30″N; 1068 to 1309 m elevation; 8.27 km^2, Figure 1) of Ansai Soil and Water Conservation Station, Chinese Academy of Sciences (CAS) and Ministry of Water Resources (MWR). The mean annual temperature at the station is 8.8°C and mean annual precipitation is 505 mm. The study area is located in the typical loess hilly and gully region of the Loess Plateau. The soil is silt loam loess; climate is temperate, semi-arid; and vegetation type belongs to forest-steppe zone. In this area, serious soil erosion is caused primarily by human activities, which has important significance for conserving soil and water resources in the region.

Sites selection

Abandoned farmlands in different ages of natural restoration were selected in the Zhifanggou small watershed. The natural restoration age of the abandoned farmland was confirmed by consulting the village elders and scientists at the station. The slope aspect, slope gradient, elevation, soil type, and previous farming practices of the selected sites were similar to minimize the effects of these factors on experimental results. All the sites have a similar loessial loam soil. The selected sites have been abandoned for 3, 10, 18, 28, and 37 years. For comparison, one site was selected as a baseline or control in slope farmland planted in soybean. Vegetation of the abandoned farmlands were all annual or perennial herbs. Land-use and vegetation information for selected sites are listed in Table I.

Soil and sampling

Soil bulk density, soil cohesion, thickness of biological crust, clay content, and soil organic matter content of each site were measured. Steel rings (5 cm in height and 5 cm in diameter) were used to determine bulk density of the top soil layer and three replicates were measured for each site. Soil strength of cohesion was measured using an Eijkelkamp pocket vane tester (14.10, Eijkelkamp Agrisearch Equipment, Giesbeek) using one of three vanes (CL100-standard: 0 to 1 kg cm^{-2}, CL101-soft: 0 to 0.2 kg cm^{-2}, or CL102-stiff: 0 to 2.5 kg cm^{-2}) selected according to the soil properties of each site. Ten replicates were tested for each site at the saturated land surface, which was sprayed slowly with a light sprayer. Thickness of the biological crust on the soil surface was measured using a caliper and ten replicates were made for each site. Six soil samples of the top 20 cm of soil were collected in an 'S'-shaped pattern for each site,

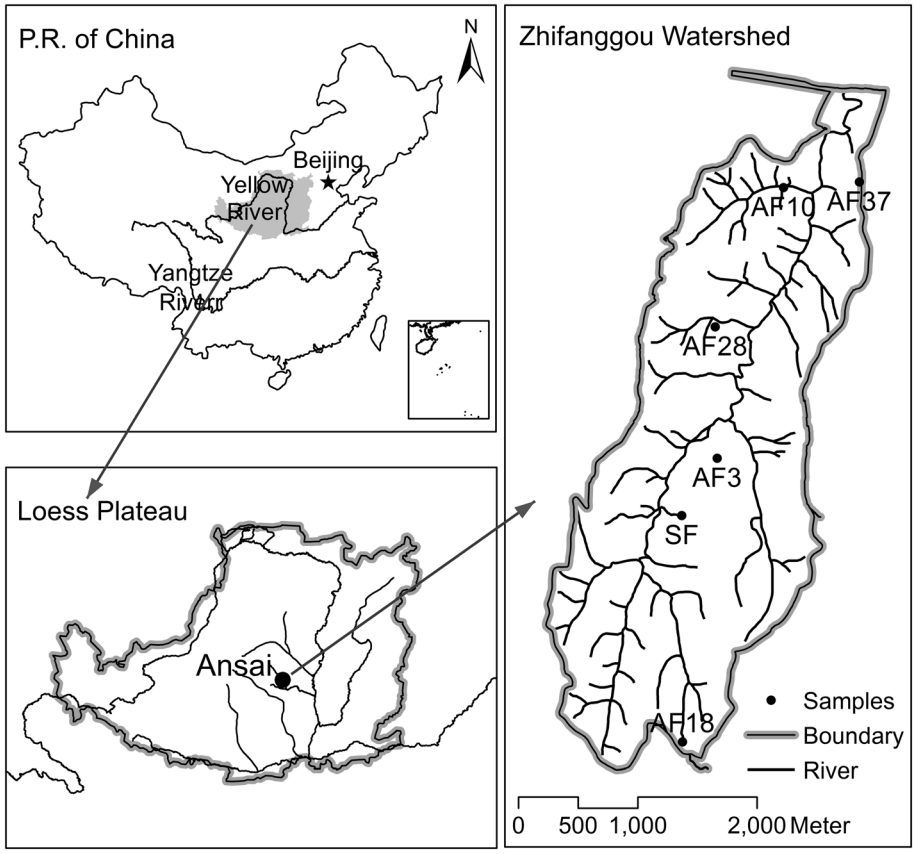

Figure 1. Location of study area.

Table I. Basic information of land use, topography, and vegetation for the sampling sites

Site code	Age (yr)	Landform	Slope (%)	Elevation (m)	Vegetation coverage (%)	Dominant communities
SF	0	hillside	8.7	1194	38.9	*soybean*
AF3	3	hillside	14.0	1184	42.3	*Achillea capillaris*
AF10	10	hillside	12.2	1089	40.9	*Achillea capillaris-Artemisia sacrorum*
AF18	18	hillside	14.0	1342	56.1	*Artemisia sacrorum- Stipa bungeana*
AF28	28	hillside	17.5	1167	60	*Artemisia sacrorum- Stipa bungeana*
AF37	37	hillside	10.5	1213	60.7	*Stipa bungeana-Artemisia sacrorum*

[a] SF is slope farmland.
[b] AF is abandoned farmlands, and the number is the abandonment age in years.
[c] All soils type are loessial soil

then well-mixed and air-dried. Roots and other debris were removed for each combined sample with a 2 mm sieve. The sieved soil samples were stored for laboratory analysis of soil particle size distribution (hydrometer method) and soil organic matter (potassium dichromate colorimetric method). The basic soil properties data are shown in Table II.

Iron rings (5 cm in height and 9.8 cm in diameter) were used to collect intact soil samples from the surface soil layer for detachment capacity measurement by overland flow. The sampling process was the same as in previous studies and can be found in Zhang *et al*. (2003, 2008a, 2009). Thirty-three samples were collected for each site and wetted for 8 h (the water level was increased gradually and the final water level was 1 cm below the soil surface) in a metal container, and then drained for 12 h and weighed. Thirty of them were used to determine soil detachment capacities, soil erodibility, and critical shear stress under different shear stresses while the remaining three were used to measure the field water holding capacity and dry soil mass for each site. Lastly, the three cores were oven dried for 24 h to determine soil moisture and the mean value that was used to calculate the initial dry soil mass for the other thirty soil samples.

Infiltration rate measurements

Infiltration rate was measured using a CSIRO disc permeameter (Center for Environmental Mechanics, Canberra, Australia). The supply water pressure heads (ψ) was – 20 mm. The detailed measuring procedure is described by Joel and Messing (2001). For each site, infiltration rate was duplicated three times and the mean value was considered as the mean infiltration rate.

The initial infiltration rate and steady infiltration rate were calculated as follows:

$$f_0 = \frac{h_0 D_2^2}{t_0 D_1^2 (0.7 + 0.03T)} \quad (1)$$

Table II. Selected soil physical and biological properties on each site

Site	Soil bulk density (kg m^{-3})	Soil cohesion (Pa)	Soil texture			Soil organic carbon (g kg^{-1})	Biological crust thickness (mm)	Root mass density (kg m^{-3})
			Clay	Slit	Sand			
			%	%	%			
SF	1250	10257	15.96	63.83	20.21	4.63	-	0.29
AF3	1247	11050	15.96	57.85	26.19	3.24	2.99	1.12
AF10	1267	10290	15.93	61.73	22.34	5.09	1.95	4.35
AF18	1239	9839	11.93	59.65	28.42	4.14	1.56	2.82
AF28	1188	10310	9.97	63.83	26.19	4.56	1.97	4.18
Af37	1186	8781	11.95	59.73	28.33	6.12	1.35	6.35

[a] SF means slope farmland.
[b] AF is abandoned farmlands, and the number is the abandonment age in years.
[c] All sites have similar loam soil texture.

where f_0 is the initial infiltration rate at 10°C standard water temperature for the first 3 min (mm min^{-1}), h_0 is the water level drop height of the reservoir for the first 3 min (mm), t_0 is the infiltration time ($t_0 = 180$ s), D_1 is the diameter of base disk ($D_1 = 200$ mm), D_2 is the diameter of reservoir ($D_2 = 47$ mm), T is the mean water temperature for the first 3 min (°C).

$$f_s = \frac{\Delta h D_2^2}{\Delta t D_1^2 (0.7 + 0.03T)} \tag{2}$$

where f_s is the steady infiltration rate at 10°C standard water temperature (mm min^{-1}), Δh (mm) is the water level drop height of reservoirs for a certain time (Δt, s), T is the water temperature (°C). The initial infiltration rate and steady infiltration rate of each site are shown in Table III.

Hydraulic parameter determination

The soil detachment capacity was measured in a 4.0 m long and 0.35 m wide flume, as used in previous studies by Zhang *et al.* (2003, 2008a, 2009). The test soil collected from the farmland was glued on to the flume bed surface, and the surface remained constant during the whole experiment process so that the hydraulic roughness was similar to that of the soil sample surfaces. The flow discharge was calibrated to the desired rate in the flume outlet with a plastic bucket and a scale prior to test. The volume of water in the bucket was accurately measured with a graduated cylinder. For a given combination of flow discharge and slope gradient, flow velocity was measured 12 times using a fluorescent dye method and modified by a reduction factor according to flow regime (Luk and Merz, 1992). The mean velocity was used to compute the flow depth h (m):

$$h = \frac{Q}{vB} \tag{3}$$

where Q is the flow discharge (m^3 s^{-1}), v is the flow velocity (m s^{-1}), and B is the flume width ($B = 0.35$ m). The mean flow depth varied from 0.003 to 0.005 m. The flow shear stress (τ, Pa) was calculated as:

$$\tau = \rho g h S \tag{4}$$

where p is the density of water (kg m^{-3}), g is the constant of gravity (m s^{-2}), and S is the slope gradient (m m^{-1}). Six combinations of unit width discharge (ranged from 0.003 to 0.007 m^2 s^{-1}) and flume bed gradient (from 17.4 to 42.3%) were tested, resulting in shear stresses of 5.83, 8.69, 11.31, 13.67, 15.73, and 18.15 Pa.

Table III. Selected infiltration rate on each site

	Initial infiltration rate (mm min^{-1})	Steady infiltration rate (mm min^{-1})
SF	1.25	0.43
AF3	1.41	0.62
AF10	1.21	0.50
AF18	1.28	0.74
AF28	1.42	0.77
Af37	1.67	0.78

[a] SF means slop farmland.
[b] AF is abandoned farmlands, and the number is the abandonment age in years.
[c] All sites have similar loam soil texture.

Measurement of detachment capacity

The flume gradient and water discharge rate were adjusted to the desired values. The wetted sample was set into a hole in the flume bed (0.5 m from the flume outlet), and was scoured under the desired flow shear stress and ended until a certain scouring depth was reached to standardize the influence of the ring rim (Nearing *et al.*, 1991; Zhang *et al.*, 2002). The scouring time varied from 15.04 to 316.70 s. Soil detachment capacity was calculated as follows:

$$D_C = \frac{w_b - w_e}{t \times A} \tag{5}$$

where D_C is the soil detachment capacity (kg s^{-1} m^{-2}), w_b is the dry weight of soil sample (kg) before the detachment test, w_e is the dry weight of the soil sample (kg) after the test (oven-drying for 24 h at 105°C), t is the test period (s), and A is the section area of the soil sample (m^2). Five samples were tested under each shear stress condition. The average value was deemed the mean detachment capacity for that shear stress. Altogether, 180 soil samples were tested. After that, soil root of each core was measured by watering and weighing (oven-drying for 24 h at 65°C), and the root mass density (kg m^{-3}) was calculated by dividing the root weight (kg) by the ring volume (3.77×10^4 m^{-3}).

Soil erodibility of rill (K_r) and critical shear stress (τ_c) were important parameters to reflect the soil resistance to erosive forces (Nearing *et al.*, 1988; Zhang *et al.*, 2002). Soil erodibility (K_r) and critical shear stress (τ_c) were estimated as the slope and intercept

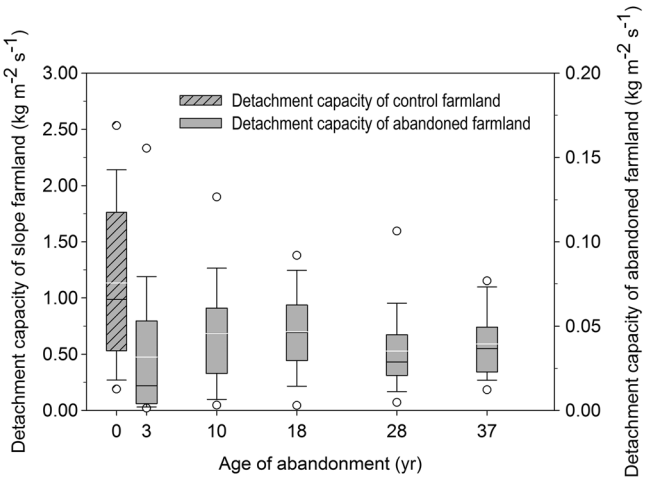

Figure 2. Mean measured soil detachment capacity for different sites (at 5th/95th percentiles).

on the *x* axis of the linear regression line between the soil detachment capacity and shear stress as described in the WEPP (water erosion prediction project) model (Nearing *et al.*, 1989).

Statistical analysis

Descriptive statistics were used to analyze soil detachment capacities between sites or restoration age groups. The relationships between soil detachment capacities, hydraulic parameters and soil properties were analyzed by a simple regression method. The relationship between soil detachment capacity and all factors (both hydraulic parameters and soil properties) was analyzed by a stepwise regression method, and the coefficient of determination and Nash–Sutcliffe efficiency (Nash and Sutcliffe, 1970) were used to evaluated the goodness of simulated results. All analyses were carried out with the SPSS package 18.0 (SPSS 18.0, Chicago, 2009).

Results and Discussion

The measured soil detachment capacity fluctuated with abandonment time (Figure 2). Soil detachment capacity of the slope farmland was significantly greater than those of the abandoned farmlands. The mean value of soil detachment capacity in the slope farmland was 24.1 to 35.4 times greater than those in the abandoned (naturally restored) farmlands (Table IV). The differences in soil detachment capacity between the slope and abandoned farmlands were probably caused by farming activities, which disturbed the soil surface and enhanced soil detachment (Zhang *et al.*, 2009). After abandonment of slope farmlands, the farming disturbance ceased and soil began to form aggregate and consolidate gradually. The resistance of soil to erosion increased, causing soil detachment capacity to decrease. For abandoned farmlands with different restoration ages, the measured detachment capacity varied with chronological series. The average soil detachment capacity increased gradually from 0.032 to 0.047 kg m^{-2} s^{-1} when the restoration age was less than 18 years and then decreased continually to 0.039 kg m^{-2} s^{-1} by the restoration age of 37 years (Table IV).

The reduction of soil detachment capacity following slope farmland abandonment also resulted from vegetation recovery. Due to the vegetation restoration in abandoned farmlands, which was considered as a process of secondary succession (Pugnaire *et al.*, 2006), runoff generation was reduced by the interception of plant and the increased soil infiltration rates (García-Ruiz and Lana-Renault, 2011). In China, as a result of the implementation of the 'Grain for Green' project, the runoff was reduced by 18% after vegetation recovery (Deng *et al.*, 2012). In the Loess Plateau, the runoff generation in abandoned farmland is reduced by 30% to 62.4% compared with that in the slope farmland due to the improved soil infiltration capacity (Hou and Zou, 1987; Hou and Cao, 1990). In this study, the infiltration rate (both initial infiltration rate and steady infiltration rate) of abandoned farmland increased with the restoration chronosequence when the age of abandonment was greater than 10 years (Table III). The fluctuation in infiltration rate during the early stage of natural vegetation succession was probably caused by the process of consolidation (Liu *et al.*, 2012). The initial infiltration rate and steady infiltration rate in 37-years-old abandoned farmland were 1.3 and 1.8 times greater than that in control farmland. Soil infiltration increases with root mass density ($P < 0.01$; Table V), although it was negatively or not correlated with biological soil crust thickness ($P < 0.05$ or $P > 0.05$; Table V). The overland flow for a given rainfall event declines as soil infiltration rate increases with abandoning age, which certainly leads to further decrease in soil detachment capacity of abandoned farmland (Zhang *et al.*, 2002, 2003).

Soil detachment by overland flow decreased with soil cohesion (De Roo *et al.*, 1996; Torri *et al.*, 1998; Zhang *et al.*, 2008), which increased with root density (Comino and Marengo, 2010: Comino *et al.*, 2010; Du *et al.*, 2010). Nevertheless, no significant correlation was found between soil cohesion and soil detachment capacity in this study. The effects of abandon age on soil detachment were complex and influenced by many factors of soil properties or vegetation characteristics except soil cohesion (Table V). However, the measured depth of the pocket vane used in this study was only 5 mm, and the effects of roots on soil cohesion were probably not detected. The measured soil cohesion was closely related to soil surface characteristics such as the depth of crust (Figure 3).

Table IV. Statistical parameters of measured soil detachment capacity (D_C)

Site code	*n*	Mean ($kgm^{-2}s^{-1}$)	Minimum ($kgm^{-2}s^{-1}$)	Maximum ($kgm^{-2}s^{-1}$)	Standard error ($kgm^{-2}s^{-1}$)	Coefficient of variation
SF	30	1.132^{A}	0.187	2.627	0.132	0.638
AF3	30	0.032^{B}	0.001	0.228	0.008	1.438
AF10	30	0.046^{B}	0.002	0.170	0.006	0.752
AF18	30	0.047^{B}	0.001	0.094	0.004	0.513
AF28	30	0.035^{B}	0.004	0.107	0.004	0.679
Af37	30	0.039^{B}	0.006	0.080	0.003	0.481

[a] SF means slope farmland.
[b] AF is abandoned farmlands, and the number is the abandonment age in years.
[c] The same letter means there is no difference between them ($P > 0.05$).
[d] Coefficient of variation is the ratio of the standard deviation to mean value of detachment capacity.

Table V. Correlation results between soil detachment capacity, and soil properties and vegetation characteristics

	Initial nfiltration	Steady infiltration	Soil cohesion	Soil bulk density	Clay content	Soil organic carbon	Biological crust thickness	Root mass density
Detachment capacity	−0.324	−0.617**	0.094	0.371*	0.384*	0.004	−0.733**	−0.517**
Initial infiltration		0.653**	−0.592**	−0.809**	−0.393*	0.474**	−0.235	0.531**
Steady infiltration			−0.548**	−0.635**	−.893**	0.221	−0.475**	0.533**
Soil cohesion				0.066	0.496**	−0.862**	0.897**	−0.733**

*Correlation is significant at the 0.05 level.
**Correlation is significant at the 0.01 level (2-tailed).

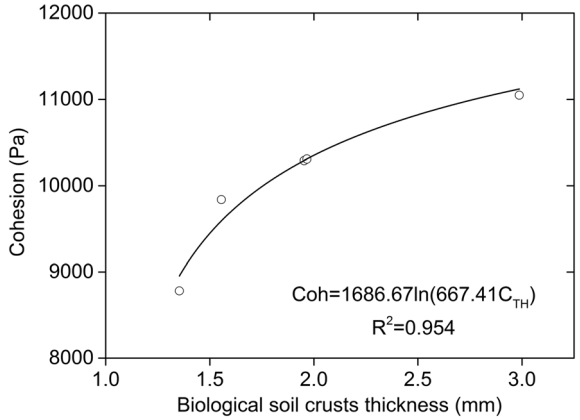

Figure 3. Soil cohesion (*Coh*) as a function of biological soil crusts thickness (C_{TH}).

Plant root networks and depth distribution were probably related to the fluctuation in soil detachment capacities. Well-developed root networks could bind soil particles and soil aggregates together and increase the soil's resistance to erosion. The root mass density of the 37-years-old abandoned farmland was the maximum value among the slope and other abandoned farmlands. It was 21 times greater than the control farmland, and 1.5 to 5.7 times greater than other abandoned farmlands. Soil detachment capacity decreased as an exponential function of root mass density ($P < 0.000$, $R^2 = 0.901$, Figure 4):

$$D_C = 5.809 \exp(-5.851 R_{MD}) \quad (6)$$

where D_C is the soil detachment capacity (kg m^{-2} s^{-1}), and R_{MD} is the root mass density (kg m^{-3}).

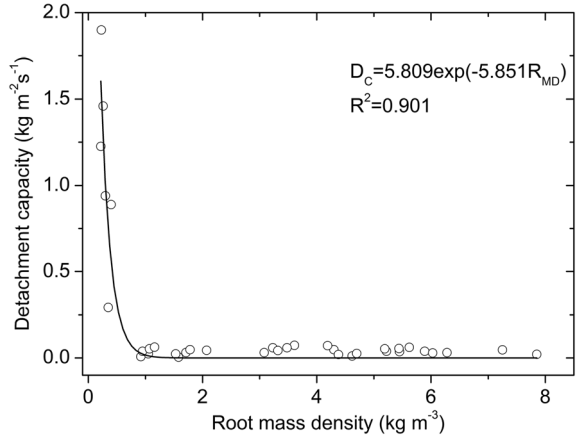

Figure 4. Soil detachment capacity (D_C) as a function of root mass density (R_{MD}).

Biological crust composed mostly of moss was another important factor influencing the soil detachment process in the idled farmlands. The biological crust quickly developed in the initial stage of restoration due to the low vegetation and litter cover, and was effective in protecting the surface soil from flow detachment (Muscha and Hild, 2006; Rodríguez-Caballero *et al.*, 2012). The biological crust of a 3-year abandoned farmland was the thickest among the studied sites and was 1.5 to 2.2 times greater than the other abandoned farmlands. The thickness of biological crust decreased gradually with increasing vegetation coverage as restoration age increased. As a result, the potential effects of biological crust on soil detachment were reduced (Rodríguez-Caballero *et al.*, 2012). The relationship between soil detachment capacity and biological crust thickness could be expressed well with an exponential function as follows ($P < 0.000$, $R^2 = 0.785$, Figure 5):

$$D_C = 1.117 \exp(-2.119 C_{TH}) \quad (7)$$

where C_{TH} is the biological crust thickness (mm). No significant relationship was found between soil detachment capacity and soil bulk density or clay content in this study. This result was probably caused by small ranges of measured soil bulk density and clay content of sites for soil sample collected.

Soil detachment increased with shear stress as a power function for all experimental sites. The coefficients of determination were greater than 0.902 and the Nash–Sutcliffe efficiencies were greater than 0.915 (Table VI). This result agreed with the report of previous studies by Zhang *et al.* (2008a) and the technology of WEPP model (Nearing *et al.*, 1988). For the dataset of all the restoration age groups, the regression result was

$$D_c = 0.001 \tau^{1.330} \quad (8)$$

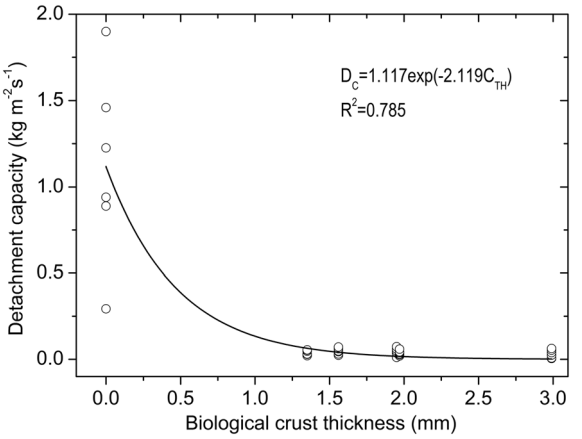

Figure 5. Soil detachment capacity (D_C) as a function of biological crust thickness (C_{TH}).

Table VI. Results of nonlinear regression between soil detachment capacity (D_C) and shear stress (τ) for different sites

Site	Power equation	R^2	p	NSE	n
SF	$D_C = 0.028\tau^{1.460}$	0.926	0.001	0.953	30
AF3	$D_C = 0.0001\tau^{2.484}$	0.947	0.001	0.965	30
AF10	$D_C = 0.001\tau^{1.479}$	0.902	0.002	0.930	30
AF18	$D_C = 0.005\tau^{0.953}$	0.974	0.000	0.941	30
AF28	$D_C = 0.004\tau^{0.870}$	0.927	0.001	0.915	30
AF37	$D_C = 0.005\tau^{0.861}$	0.924	0.001	0.935	30
Abandoned farmlands	$D_C = 0.001\tau^{1.330}$	0.835	0.000	0.830	150

[a] SF refers to slope farmland.
[b] AF is abandoned farmlands, and the number is the abandonment age in years.

The coefficient of determination and Nash–Sutcliffe efficiency were 0.835 and 0.830, respectively. Equation (8) was compared with the results of a wasteland (idled marginal land) and 8-year-old grassland reported by Zhang *et al.* (2008a) in Figure 6. Although soil type was similar and all plots were clipped, the predicted results were quite different when shear stress was greater than 8 Pa (Figure 6). Soil detachment capacity of the wasteland and 8-year-old grassland increased faster than that of the abandoned farmland. The differences are probably caused by differences in vegetation and biological crust characteristics, root system and restoration age. In the study by Zhang *et al.* (2008a), eight-year-old *Astragalus adsuigens Pall* had tap roots and the restoration age of the idle land was shorter than most sites in this study. The tap roots of *Astragalus adsuigens Pall* were less effective in reducing soil detachment than the fibrous roots in the current study (Wischmeier, 1975; Dissmeyer and Foster, 1980; De Baets *et al.*, 2007). For the wasteland, the lower vegetation cover resulted in lower ability to reduce soil detachment capacity, compared with abandoned farmlands in this study.

Despite flow shear stress, soil detachment capacity was also influenced by biological crust, soil properties and vegetation characteristics as shown above. Hence, the relationship between soil detachment capacity and all these factors measured in this study was analyzed using a stepwise regression method. The result indicated that soil detachment capacity could be simulated with a power function as follows:

$$D_C = 0.002\tau^{1.224} C_{TH}{}^{-0.195} \quad (9)$$

Although both root mass density and biological crust thickness had close relationships with detachment capacity (Equations (6) and (7)), root mass density was not included in the function when all the hydraulic parameters, soil properties and vegetation characteristics were considered when using the method of regression analysis. The coefficient of determination was 0.851 and the Nash–Sutcliffe efficiency was 0.845 (Figure 7). Compared with Equation (8), the fitting was slightly improved.

Soil erodibility (K_r) and critical shear stress (τ_c) were important parameters reflecting soil resistance to rill erosion. Soil detachment in rills occurs when flow shear stress exceeds the critical shear stress of the soil as well as when sediment concentration is lower than sediment transport capacity of the flow. Hence, rill erodibilities and critical shear stress were normally estimated for soils of the slope and abandoned farmlands using simple linear regression based on the WEPP formulation (Nearing *et al.*, 1988) and the results were shown in Figure 8.

Soil erodibility of the slope farmland differed significantly with those of the abandoned farmlands and it was 22.8 to 40.1 times greater than those of the abandoned farmlands. After farmland was abandoned, soil erodibility decreased rapidly due to biological crust formation, natural vegetation restoration, and soil consolidation in the absence of tillage disturbance (Zhang *et al.*, 2009). Soil erodibility of 3-year-old abandoned farmland declined by 95.6% compared with the slope farmland. With natural vegetation restoration and increases in species diversity, soil erodibility of the abandoned farmland decreased gradually with restoration age, and tended to stabilize 28 years after abandonment (Figure 9). Soil erodibility of 28-year-old abandoned farmland was 41.2% lower than that of 3-year-old abandoned farmland, and was similar to that of 37-year-old abandoned farmland. Erodibilities of the abandoned farmlands of this study ranged from 0.003 to 0.005 s m^{-1}, which were 37.7% to 62.9%, and 35.7% to 59.5% of those reported by Zhang *et al.* (2003) and Nearing *et al.* (1999), respectively, but were one order greater than those reported by Laflen *et al.* (1991). These differences were probably caused by differences in land use, vegetation, soil, and surface properties. The soil samples were taken from a farmland planted with soybean in the work of Zhang *et al.* (2003), and from a stony hillslope in Nearing *et al.* (1999), but from the undisturbed abandoned farmlands of a loess soil with restored vegetation and biological crusts in this study. Soil erodibilities reported by Laflen *et al.* (1991) were obtained from runoff plot data of simulated rainfall, and the methodology was quite different from the other three studies in which the data were obtained using inflow.

Critical shear stress of the abandoned farmlands changed from 0.051 to 5.980 Pa (Figure 10), which were 2.3 to 273.1%, 1.3 to 149.9%, and 1.0 to 119.6% of those reported by Zhang

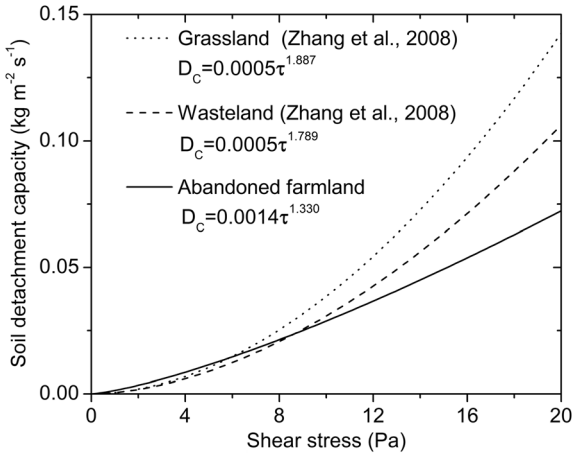

Figure 6. Comparison of relationships between detachment capacity (D_C) and shear stress (τ) proposed in this and previous studies.

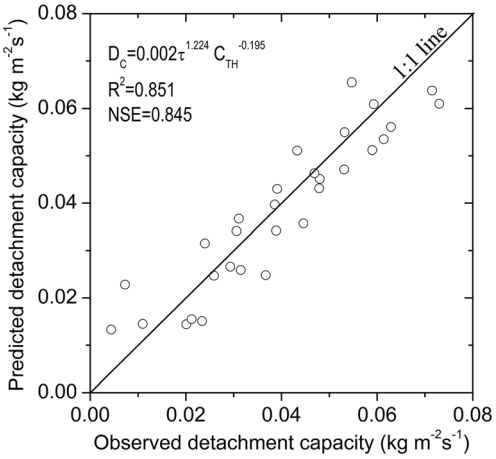

Figure 7. Comparison between observed and predicted detachment capacity.

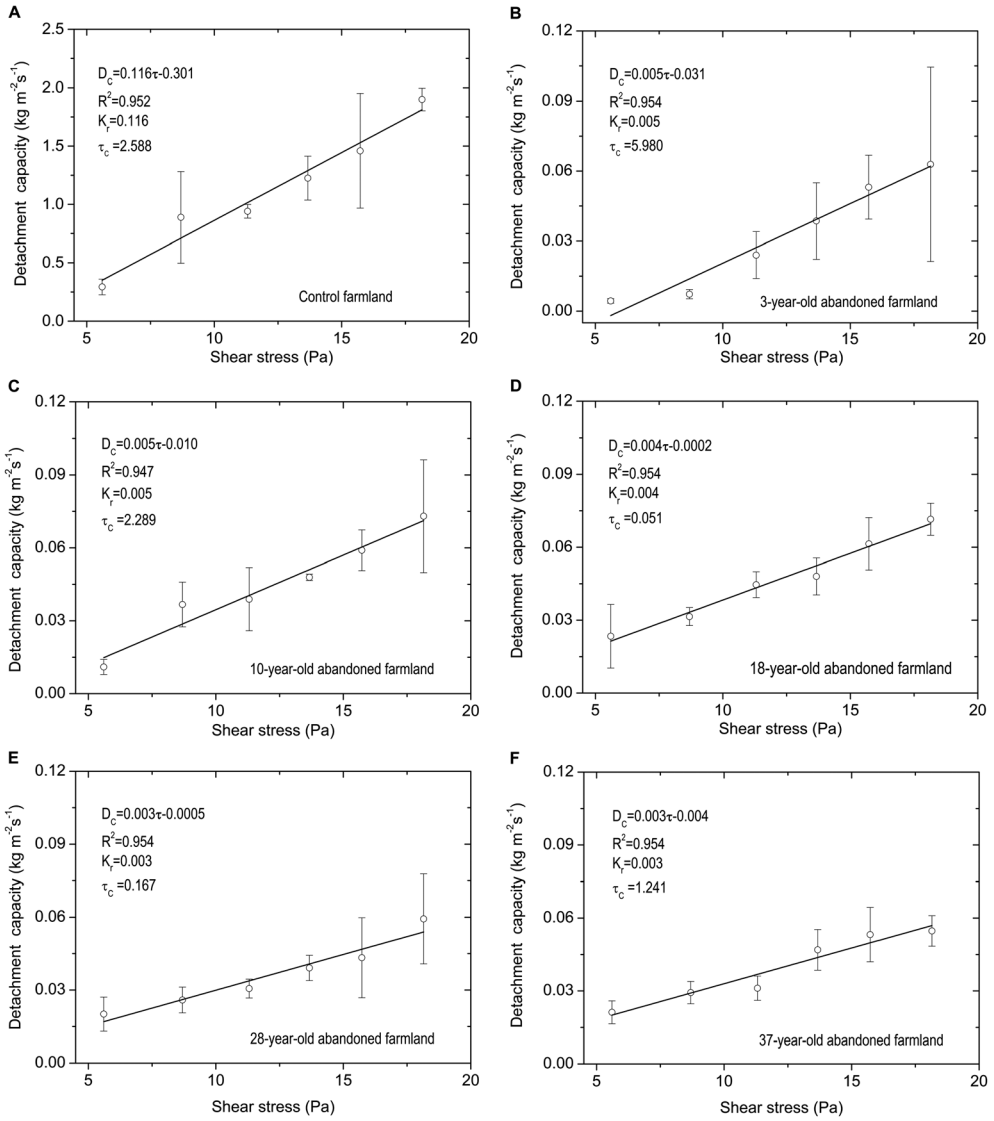

Figure 8. Soil detachment capacity (D_C) as a function of shear stress (τ).

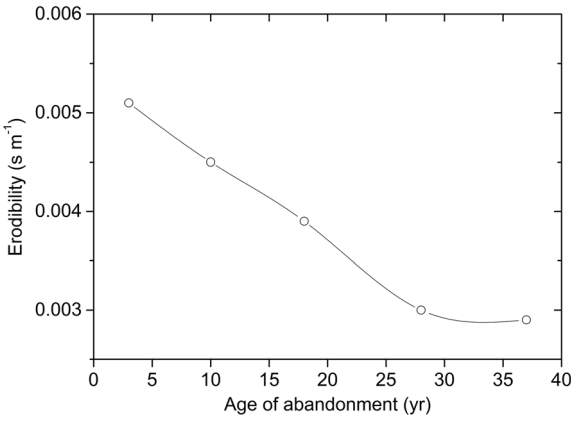

Figure 9. Variation in soil erodibility with restoration age.

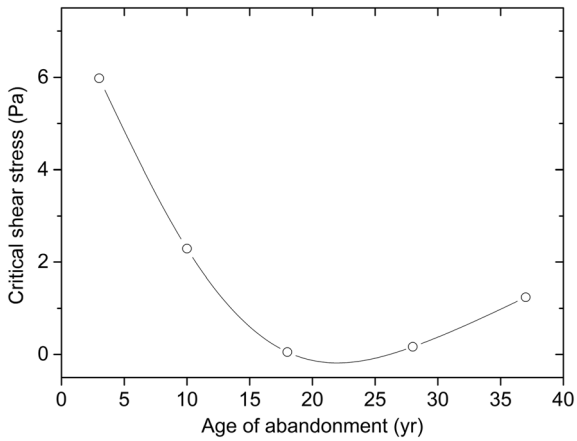

Figure 10. Variation in critical shear stress with restoration age.

et al. (2002, 2003) and Nearing *et al.* (1999), respectively. It varied with restoration age in a non-monotonic fashion, reaching the minimum around the abandonment age of 18. The farmland abandoned for 3 years had the maximum critical shear stress. It was 2.3 times greater than slope farmland, and 2.6 to 116.6 times greater than the other abandoned farmlands. The non-monotonic change pattern in critical shear stress was probably caused by inherent heterogeneity among soil samples or by the slight difference in soil properties and vegetation characteristics of the sampling points. Further analysis indicated that critical shear stress increased with an increase in thickness of biological crust ($P = 0.026$, $R^2 = 0.806$):

$$\tau_C = 0.109 C_{TH}^{-3.651} \quad (10)$$

where τ_c is the critical shear stress (Pa). The close correlation between critical shear stress and biological crust thickness reflected the complex relationship between soil detachment capacity and restoration age. This result indicated that the biological crust thickness played an important role in reducing soil detachment. Further studies are needed to quantify the relationship between soil detachment capacity and biological crust thickness to understand the mechanism of soil erosion during the progression of natural vegetation restoration in the Loess Plateau.

Conclusions

Soil erosion in the Loess Plateau could be greatly reduced by implementing natural vegetation restoration. This study was undertaken to assess the effects of age of farmland abandonment under natural vegetation restoration on soil detachment capacity and soil resistance to erosion using undisturbed soil samples collected from one slope and five abandoned farmlands in one typical small watershed located in the central Loess Plateau. The results indicated that soil detachment capacity by overland flow decreased significantly after slope farmland was abandoned for natural vegetation restoration. The mean detachment capacity of the currently cultivated slope farmland was 24.1 to 35.4 times greater than that of the abandoned farmlands, which, to some extent, demonstrates the benefits of vegetation and biological crust in reducing soil loss. Soil detachment was significantly influenced by shear stress, root mass density and thickness of biological crust, and it could be simulated well by flow shear stress and biological crust thickness with a power function (NSE = 0.851). Soil erodibility decreased with restoration age and gradually leveled off after 28 years of natural restoration. The critical shear stress of the abandoned farmland varied non-monotonically with restoration age, probably due to evolution in biological crusts and vegetation composition. Further studies, in the Loess Plateau, are needed to quantify the relationship between soil detachment capacity and biological crust thickness to better understand the mechanism of soil detachment during the progression of natural vegetation restoration.

Acknowledgements—Financial assistance for this work was provided by the Hundred Talents Project of the Chinese Academy of Sciences, the National Natural Science Foundation of China (No.41271287), and the Open Fund from State Key Laboratory of Soil Erosion and Dryland Farming on the Loess Plateau (K318009902-1313). The authors thank the members of the Ansai Research Station of Soil and Water Conservation, Chinese Academy of Sciences and Ministry of Water Recourses for technical assistance.

References

Chen L, Gong J, Fu B, Huang Z, Huang Y, Gui L. 2007. Effect of land use conversion on soil organic carbon sequestration in the loess hilly area, loess plateau of China. *Ecological Research* **22**: 641–648.

Cochrane TA, Flanagan DC. 1997. Detachment in a simulated rill. *Transactions of ASAE* **40**: 111–119.

Comino E, Marengo P. 2010. Root tensile strength of three shrub species: Rosa canina, Cotoneaster dammeri and Juniperus horizontalis soil reinforcement estimation by laboratory tests. *Catena* **82**: 227–235.

Comino E, Marengo P, Rolli V. 2010. Root reinforcement effect of different grass species: a comparison between experimental and models results. *Soil and Tillage Research* **110**: 60–68.

De Baets S, Poesen J, Gyssels G, Knapen A. 2006. Effects of grass roots on the erodibility of topsoils during concentrated flow. *Geomorphology* **76**: 54–67.

De Baets S, Poesen J, Knapen A, Galindo P. 2007. Impact of root architecture on the erosion-reducing potential of roots during concentrated flow. *Earth Surface Processes and Landforms* **32**: 1323–1345.

De Roo APJ, Wesseling CG, Ritsema CJ. 1996. LISEM: A single-event physically based hydrological and soil erosion model for drainage basins. I. Theory, input and output. *Hydrological Processes* **10**: 1107–1117.

Deng L, Shangguan ZP, Li R. 2012. Effects of the grain-for-green program on soil erosion in China. *International Journal of Sediment Research* **27**: 120–127.

Dissmeyer GE, Foster GR. 1980. A guide for predicting sheet and rill erosion on forest land. US Department of Agriculture Forest Service, Atlanta, GA.

Du Q, Zhong QC, Wang KY. 2010. Root effect of three vegetation types on shoreline stabilization of Chongming Island, Shanghai. *Pedosphere* **20**: 692–701.

Fu B, Gulinck H. 1994. Land evaluation in an area of severe erosion: the Loess Plateau of China. *Land Degradation and Development* **5**: 33–40.

Fu B, Chen L, Ma K, Zhou H, Wang J. 2000. The relationships between land use and soil conditions in the hilly area of the Loess Plateau in northern Shaanxi, China. *Catena* **39**: 69–78.

García-Ruiz JM, Lana-Renault N. 2011. Hydrological and erosive consequences of farmland abandonment in Europe, with special reference to the Mediterranean region – a review. *Agriculture, Ecosystems and Environment* **140**: 317–338.

Ghebreiyessus YT, Gantzer CJ, Alberts EE. 1994. Soil-erosion by concentrated flow-shear-stress and bulk-density. *Transactions of ASAE* **37**: 1791–1797.

Govers G, Everaert W, Poesen J, Rauws G, De Ploey J, Lautridou JP. 1990. A long flume study of the dynamic factors affecting the resistance of a loamy soil to concentrated flow erosion. *Earth Surface Processes and Landforms* **15**: 313–328.

Govers G, Giménez R, Van Oost K. 2007. Rill erosion: exploring the relationship between experiments, modelling and field observations. *Earth-Science Reviews* **84**: 87–102.

Hairsine PB, Rose CW. 1992a. Modeling water erosion due to overland-flow using physical principles. 1. Sheet flow. *Water Resources Research* **28**: 237–243.

Hairsine PB, Rose CW. 1992b. Modeling water erosion due to overland-flow using physical principles. 2. Rill flow. *Water Resources Research* **28**: 245–250.

Hou XL, Cao QY. 1990. Study on the benefits of plants to reduce sediment in the Loess rolling gullied region of north Shaanxi. *Bulletin of Soil and Water Conservation* **10**: 33–40.

Hou XL, Zou HY. 1987. Investigation report of vegetation and its effects on reducing sediment yield in Ansai soil and water experiment plot. *Journal of Sediment Research* **4**: 98–102.

Hu W, Shao MA, Wang QJ, Fan J, Reichardt K. 2008. Spatial variability of soil hydraulic properties on a steep slope in the Loess Plateau of China. *Scientia Agricola* **65**: 268–276.

Jiang Y, Kang M, Gao Q, He L, Xiong M, Jia Z, Jin Z. 2003. Impact of land use on plant biodiversity and measures for biodiversity conservation in the Loess Plateau in China – a case study in a hilly-gully region of the northern Loess Plateau. *Biodiversity and Conservation* **12**: 2121–2133.

Jiao J, Tzanopoulos J, Xofis P, Bai W, Ma X, Mitchley J. 2007. Can the study of natural vegetation succession assist in the control of soil erosion on abandoned croplands on the Loess Plateau. *China Restoration Ecology* **15**: 391–399.

Joel A, Messing I. 2001. Infiltration rate and hydraulic conductivity measured with rain simulator and disc permeameter on sloping arid land. *Arid Land Research and Management* **15**: 371–384.

Khanbilvardi RM, Rogowski AS. 1986. Modeling soil-erosion, transport and deposition. *Ecological Modelling* **33**: 255–268.

Knapen A, Poesen J, Govers G, De Baets S. 2008. The effect of conservation tillage on runoff erosivity and soil erodibility during concentrated flow. *Hydrological Processes* **22**: 1497–1508.

Laflen JM, Elliot WJ, Simanton JR, Holzhey CS, Kohl KD. 1991. WEPP - soil erodibility experiments for rangeland and cropland soils. *Journal of Soil and Water Conservation* **46**: 39–44.

Li G, Luk SH, Cai QG. 1995. Topographic zonation of infiltration in the hilly Loess region, North China. *Hydrological Processes* **9**: 227–235.

Li Y, Shao M. 2006. Change of soil physical properties under long-term natural vegetation restoration in the Loess Plateau of China. *Journal of Arid Environments* **64**: 77–96.

Li Y, Zhu XM, Tian JY. 1991. Effectiveness of plant roots to increase the anti-scourability of soil on the Loess Plateau. *Chinese Science Bulletin* **36**: 2077–2082.

Li Z, Zheng FL, Liu WZ. 2012. Spatiotemporal characteristics of reference evapotranspiration during 1961–2009 and its projected changes during 2011–2099 on the Loess Plateau of China. *Agricultural and Forest Meteorology* **154–155**: 147–155.

Liu G, Xu M, Ritsema C. 2003. A study of soil surface characteristics in a small watershed in the hilly, gullied area on the Chinese Loess Plateau. *Catena* **54**: 31–44.

Liu Y, Fu BJ, Lu YH, Wang Z, Gao GY. 2012. Hydrological responses and soil erosion potential of abandoned cropland in the Loess Plateau, China. *Geomorphology* **138**: 404–414.

Luk SH, Merz W. 1992. Use of the slat tracing technique to determine the velocity of overlan-flow. *Soil Technology* **5**: 289–301.

Mamo M, Bubenzer G. 2001a. Detachment rate, soil erodibility, and soil strength as influenced by living plant roots. Part I. Laboratory study. *Transactions of ASAE* **44**: 1167–1174.

Mamo M, Bubenzer G. 2001b. Detachment rate, soil erodibility, and soil strength as influenced by living plant roots. Part II. Field study. *Transactions of ASAE* **44**: 1175–1181.

Morgan RPC, Quinton JN, Smith RE, Govers G, Poesen JWA, Auerswald K, Chisci G, Torri D, Styczen ME. 1998. The european soil erosion model (EUROSEM): a dynamic approach for predicting sediment transport from fields and small catchments. *Earth Surface Processes and Landforms* **23**: 527–544.

Muscha JM, Hild AL. 2006. Biological soil crusts in grazed and ungrazed Wyoming sagebrush steppe. *Journal of Arid Environments* **67**: 195–207.

Nash JE, Sutcliffe JV. 1970. River flow forecasting through conceptual models. Part I. A discussion of principles. *Journal of Hydrology* **10**: 282–290.

Nearing MA, Bradford JM, Parker SC. 1991. Soil detachment by shallow flow at low slopes. *Soil Science Society of America Journal* **55**: 339–344.

Nearing MA, Foster GR, Lane LJ, Finkner SC. 1989. A process-based soil-erosion model for USDA-water erosion prediction project technology. *Transactions of ASAE* **32**: 1587–1593.

Nearing MA, Simanton JR, Norton LD, Bulygin SJ, Stone J, USDA A. 1999. Soil erosion by surface water flow on a stony, semiarid hillslope. *Earth Surface Processes and Landforms* **24**: 677–686.

Nearing MA, West LT, Brown LC. 1988. A consolidation model for estimating changes in rill erodibility. *Transactions of ASAE* **31**: 696–700.

Pugnaire FI, Luque MT, Armas C, Gutiérrez L. 2006. Colonization processes in semiarid Mediterranean old-fields. *Journal of Arid Environments* **65**: 591–603.

Rodríguez-Caballero E, Cantón Y, Chamizo S, Afana A, Solé-Benet A. 2012. Effects of biological soil crusts on surface roughness and implications for runoff and erosion. *Geomorphology* **145–146**: 81–89.

SPSS 18.0. 2009. *Statistical Package for the Social Sciences (SPSS) version 18.0 for Windows*. SPSS Inc.: Chicago, USA.

Torri D, Ciampalini R, Gil PA. 1998. The role of soil aggregates in soil erosion processes. In *Modelling Soil Erosion by Water*, Boardman J, Favis-Mortlock D (eds). Springer Verlag: Berlin/Heidelberg; 247–258.

Wang B, Liu GB, Xue S, Zhu BB. 2011. Changes in soil physico-chemical and microbiological properties during natural succession on abandoned farmland in the Loess Plateau. *Environmental Earth Sciences* **62**: 915–925.

Wischmeier WH. 1975. Estimating the soil loss equation's cover and management factor for undisturbed areas. In *Present and Prospective Technology for Predicting Sediment Yields and Sources*. Workshop Oxford: Mississippi; 118–124.

Xu M, Zhao Y, Liu G, Wilson G. 2006. Identification of soil quality factors and indicators for the Loess Plateau of China. *Soil Science* **171**: 400–413.

Zhang GH, Liu BY, Liu GB, He XW, Nearing MA. 2003. Detachment of undisturbed soil by shallow flow. *Soil Science Society of America Journal* **67**: 713–719.

Zhang GH, Liu BY, Nearing MA, Huang CH, Zhang KL. 2002. Soil detachment by shallow flow. *Transactions of ASAE* **45**: 351–357.

Zhang GH, Liu GB, Tang KM, Zhang, XC. 2008a. Flow detachment of soils under different land uses in the Loess Plateau of China. *Transactions of the ASABE* **51**: 883–890.

Zhang GH, Tang MK, Zhang XC. 2009. Temporal variation in soil detachment under different land uses in the Loess Plateau of China. *Earth Surface Processes and Landforms* **34**: 1302–1309.

Zhang X, Zhang L, Zhao J, Rustomji P, Hairsine P. 2008b. Responses of streamflow to changes in climate and land use/cover in the Loess Plateau, China. *Water Resources Research* **44**: 1–12.

Zhang XC, Liu WZ. 2005. Simulating potential response of hydrology, soil erosion, and crop productivity to climate change in Changwu tableland region on the Loess Plateau of China. *Agricultural and Forest Meteorology* **131**: 127–142.

Zheng FL, Huang CH, Norton LD. 2000. Vertical hydraulic gradient and run-on water and sediment effects on erosion processes and sediment regimes. *Soil Science Society of America Journal* **64**: 4–11.

Zhou ZC, Shang-Guan ZP. 2005. Soil anti-scouribility enhanced by plant roots. *Journal of Integrative Plant Biology* **47**: 676–682.

Zhu W, Cheng S, Cai X, He F, Wang J. 2009. Changes in plant species diversity along a chronosequence of vegetation restoration in the humid evergreen broad-leaved forest in the rainy zone of west China. *Ecological Research* **24**: 315–325.

